

Gas holdup and flow regime transition in spider-sparger bubble column: effect of liquid phase properties

This content has been downloaded from IOPscience. Please scroll down to see the full text.

2017 J. Phys.: Conf. Ser. 796 012041

(<http://iopscience.iop.org/1742-6596/796/1/012041>)

View [the table of contents for this issue](#), or go to the [journal homepage](#) for more

Download details:

IP Address: 131.175.12.86

This content was downloaded on 04/04/2017 at 21:04

Please note that [terms and conditions apply](#).

You may also be interested in:

[Experimental investigation of counter current air-water flow in a large diameter vertical pipe with inners](#)

Giorgio Besagni, Gaël Guédon and Fabio Inzoli

[Influence of electrolyte concentration on holdup, flow regime transition and local flow properties in a large scale bubble column](#)

Giorgio Besagni and Fabio Inzoli

[Local liquid velocity measurement in trickle bed reactors \(TBRs\) using the x-ray digital industrial radiography \(DIR\) technique](#)

Khairul Anuar Mohd Salleh, Hyoung Koo Lee and Muthanna H Al-Dahhan

[The wire-mesh sensor as a two-phase flow meter](#)

H Shaban and S Tavoularis

[Influence of void on image quality of industrial SPECT](#)

J G Park, S H Jung, J B Kim et al.

[Mathematical simulation of fluid flow in liquidsystems](#)

Lifeng Zhang

[Study on bubble sizes in a down-flow liquid jet gas pump](#)

Y L Wu, Q J Xiang, H Li et al.

[Investigation of gas–solids flow in a circulating fluidized bed using 3D electrical capacitance tomography](#)

Mingxu Mao, Jiamin Ye, Haigang Wang et al.

Gas holdup and flow regime transition in spider-sparger bubble column: effect of liquid phase properties

Giorgio Besagni*, Fabio Inzoli*, Giorgia De Guido**, Laura A. Pellegrini**

* Politecnico di Milano, Department of Energy, Via Lambruschini 4a, 20156, Milano

** Politecnico di Milano, Dipartimento di Chimica, Materiali e Ingegneria Chimica “G. Natta”, Piazza Leonardo da Vinci 32, 20133, Milano

E-mail: giorgio.besagni@polimi.it

Abstract. This paper discusses the effects of the liquid velocity and the liquid phase properties on the gas holdup and the flow regime transition in a large-diameter and large-scale counter-current two-phase bubble column. In particular, we compared and analysed the experimental data obtained in our previous experimental studies. The bubble column is 5.3 m in height, has an inner diameter of 0.24 m, it was operated with gas superficial velocities in the range of 0.004–0.20 m/s and, in the counter-current mode, the liquid was recirculated up to a superficial velocity of -0.09 m/s. Air was used as the dispersed phase and various fluids (tap water, aqueous solutions of sodium chloride, ethanol and monoethylene glycol) were employed as liquid phases. The experimental dataset consist in gas holdup measurements and was used to investigate the global fluid dynamics and the flow regime transition between the homogeneous flow regime and the transition flow regime. We found that the liquid velocity and the liquid phase properties significantly affect the gas holdup and the flow regime transition. In this respect, a possible relationship (based on the lift force) between the flow regime transition and the gas holdup was proposed.

1. Introduction

Two-phase bubble columns are equipment used for bringing one or several gases into contact with a liquid phase. They are built in several forms, but the simplest configuration consists in a vertical cylinder with no internals, in which the gas enters at the bottom through a gas distributor. The liquid phase may be supplied in batch mode or it may be led in either co-currently or counter-currently to the upward gas stream. This type of contacting devices has found many applications in the chemical, petrochemical and biochemical industries thanks to a number of advantages they provide in both design and operation (i.e., the lack of any mechanically operated parts, low energy input requirements and reasonable prices). Despite the simple column arrangement, the interactions between the phases inside the reactor are extremely complex, making their design and scale-up very difficult. Indeed, although a large amount of research is ongoing, the correct prediction of the fluid dynamics inside bubble columns is still hardly possible without experimentation. In particular, the global and local fluid dynamics in bubble columns can be described by global as well as local flow properties—i.e., the gas holdup (ϵ_G) and bubble size distribution (BSD). The gas holdup is a dimensionless parameter defined as the volume of the gas phase divided by the total volume. It determines the residence time and, in combination with the BSD, the interfacial area for the rate of interfacial mass transfer. The



global and local flow properties are related to the prevailing flow regime, which can be distinguished (in large-diameter bubble columns) in (i) the homogeneous flow regime, (ii) the transition flow regime and (iii) the heterogeneous flow regime [1]. The homogeneous flow regime—associated with small superficial gas velocities, U_G —is referred as the flow regime where only “*non-coalescence-induced*” bubbles exist (e.g. as detected by the gas disengagement technique, see ref. [2]). The homogeneous flow regime can be distinguished into “*pure-homogeneous*” (or “*mono-dispersed homogeneous*”) flow regime and “*pseudo-homogeneous*” (or “*poly-dispersed homogeneous*” or “*gas maldistribution*”) flow regime. The transition from the homogeneous flow regime toward the heterogeneous flow regime is a gradual process in which a transition flow regime occurs. The transition flow regime is identified by the appearance of the “*coalescence-induced*” bubbles and is characterized by large flow macrostructures with large eddies and a widened bubble size distribution due to the onset of bubble coalescence. At high gas superficial velocities, a fully heterogeneous flow regime is reached [3]; it is associated with high coalescence and breakage rates and a wide variety of bubble sizes. It is worth noting that, in large-diameter bubble columns, the slug flow regime may not exist because of the Rayleigh–Taylor instabilities [4]. The transitions between the three prevailing flow regimes depend on (i) the operation mode, (ii) the design parameters and (iii) the gas/liquid phases of the bubble column. For example, using a sparger that produces mainly very small bubbles the homogeneous flow regime is stabilized [5], whereas the “*mono-dispersed homogeneous flow regime*” may not exist if large bubbles are aerated [2] up to a “*pure heterogeneous flow regime*” from the beginning [6].

The many relationships between the bubble column fluid dynamic parameters and the various variables characterizing the system make it difficult to find general correlations for the precise design of bubble columns (i.e., the correct estimation of the gas holdup) [7]. Indeed, the large variation of gas holdup values presented in the literature leads to the development of a large number of correlations for the gas holdup. To this end, we have set up a large-scale and large-diameter bubble column to study the global and local bubble column fluid dynamics and, thus, to provide rational basis for bubble column design and scale-up [2]. The bubble column has a $d_c = 0.24$ m inner diameter, $H_c = 5.3$ m height ($H_c/d_c > 20$). The diameter of the column, its height and the sparger openings were chosen considering the well-known scale up criteria: generally, a diameter greater than 0.15 m, an aspect ratio larger than $H_0/d_c > 5$ (H_0 is the liquid free level) and sparger openings larger than $d_o > 1$ mm guarantee results that could be used for scaling-up [8]. In our previous papers the influence of the column and sparger design [2, 9], of the operation modes [2, 9, 10, 11, 12] and of sodium chloride (as an electrolyte) concentration [13], ethanol concentration [14] and monoethylene glycol concentration [15] over the bubble column fluid dynamics was studied. This paper summarizes and compares the previous experimental results and further discusses this topic. In particular, the relationship between the flow regime transition and the gas holdup are discussed. The present work represents the first step of a larger research framework focused on establishing a large dataset of gas holdup data to develop general gas holdup correlations. This paper is structured as follows. In Section 2 the experimental setup and dataset is described, in Section 3 the experimental results are presented and are summarized and compared in Section 4. Finally, conclusions are drawn.

2. The experimental setup and the methods

2.1. Gas holdup measurements

The experimental facility (Figure 1a) is a non-pressurized vertical pipe made of Plexiglas[®] with $d_c = 0.24$ m and $H_c = 5.3$ m. A pressure reducer controls the pressure upstream from the rotameters (1) and (2), used to measure the gas flow rate (accuracy $\pm 2\%$ f.s.v., E5-2600/h, manufactured by ASA, Italy). A pump, controlled by a bypass valve, provides water recirculation, and a rotameter (3) measures the liquid flowrate (accuracy $\pm 1.5\%$ f.s.v., G6-3100/39, manufactured by ASA, Italy). The values of gas density (used to compute the superficial gas velocity) are based upon the operating conditions existing at the column mid-point (computed by using the ideal gas law). The gas distributor, is a spider-sparger distributor (Figure 2a and 2b) with hole diameters $d_o = 2 - 4$ mm (Figure 2b). The spider sparger, has

six arms made of 0.012 m diameter stainless steel tubes soldered to the center cylinder of the sparger. The sparger was installed with the six holes located on the side of each arm facing upward. These holes are distributed with an increasing diameter moving toward the column wall (Figure 2a). The gas and liquid temperatures were checked and maintained constant at room temperature during all the experiments (22 ± 1 °C). It is worth noting that the diameter of the column, its height and the sparger openings were chosen considering the scale-up criteria listed in the introduction [8].

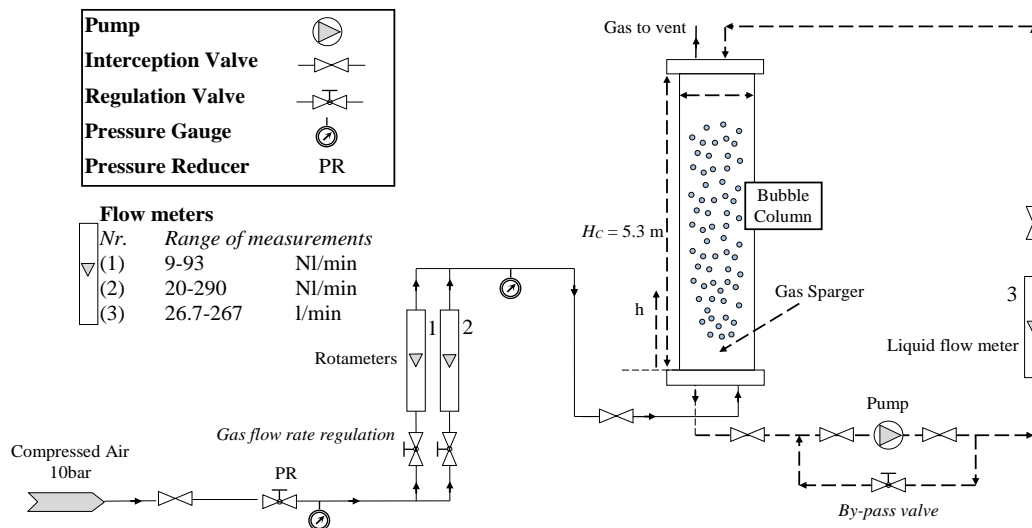
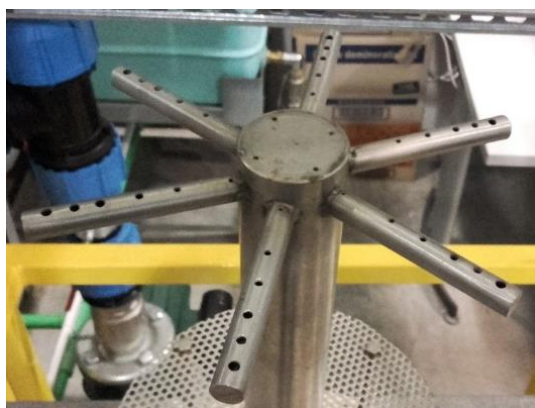
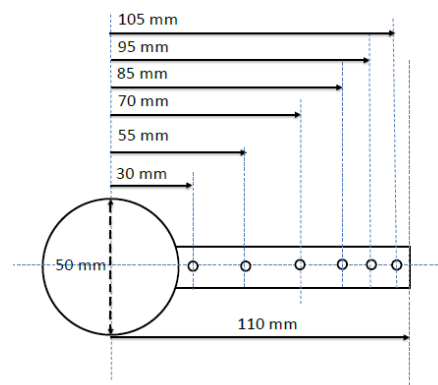


Figure 1. The experimental facility.



(a) Spider sparger: view from top



(b) Spider sparger: distribution of the openings

Figure 2. The spider sparger.

In all the runs, filtered air was used as the dispersed phase and various fluids (tap water, aqueous solutions of sodium chloride, a water-ethanol mixture and solutions of water-monoethylene glycol of different concentrations) were employed as the liquid phase to study the influence of the liquid properties on the bubble column fluid dynamics. In such a case, a liquid of a known composition was charged to the column and the gas flow rate adjusted to the desired value. The liquid phases were chosen to study the influence of organic (ethanol) and inorganic (sodium chloride) active agents, and viscous solutions:

- aqueous solution of ethanol (EtOH): 0.05% wt;

- aqueous solution of sodium chloride (NaCl): between 0.1 and 1%wt (corresponding to a concentration ratio $0.17 < c/c_t < 1.17$, Table 1; where c is the NaCl molar concentration and $c_t = 0.145$ l/mol is the critical value for the coalescence inhibition, as reported in the literature [16] and discussed in [13]).
- aqueous solution of monoethylene glycol (MEG): 11 concentrations between 0.05 and 80%wt; to investigate the “*dual effect*” of the viscosity as described by Besagni et al. [15]. The properties of the solutions tested are summarized in Table 2. The properties for pure water have been taken from those available in the literature [17-19]. As for the physical properties of water-MEG mixtures, the work by Sun and Teja [20] has been taken into account for evaluating their densities and viscosities as a function of the mass fraction of monoethylene glycol, of the temperature and of the properties of the two components constituting the binary system. As for the surface tension of aqueous monoethylene glycol solutions at 298.15 K, the correlation found in the product guide provided by MEGlobalTM [21] has been used.

Table 1. NaCl concentrations tested.

c [mol/l]	0	0.02	0.07	0.12	0.145 ¹	0.170
c/c_t [-]	0	0.14	0.48	0.84	1	1.17

¹Critical concentration, $c_t = 0.145$ mol/l [16]

Table 2. Liquid phases tested (properties evaluated at T = 25°C, p = 101325 Pa).

$c_{MEG,wt}$ [%]	ρ_L [kg/m ³]	μ_L [mPa*s]	σ [mN/m]
0	997.086	0.8903	0.0715
0.05	997.158	0.8917	0.0715
0.1	997.229	0.8928	0.0715
0.5	997.801	0.9019	0.0713
0.75	998.159	0.9077	0.0712
1	998.516	0.9135	0.0711
5	1004.208	1.0106	0.0696
8	1008.443	1.0894	0.0685
10	1011.249	1.1450	0.0677
40	1051.150	2.4287	0.0583
80	1094.801	7.9655	0.0502

2.2. Gas holdup measurements

Measurements of the bed expansion allowed the evaluation of the gas holdup ε_G . The procedure involves measuring the location (height) of liquid free surface when air flows in the column. The gas holdup is, then, obtained using the following relation:

$$\varepsilon_G = \frac{(H_D - H_0)}{H_D} \quad (1)$$

Where H_D and H_0 are the heights (measured from the sparger) of the free surface after and before aeration, respectively. The free surface before aeration is $H_0 = 3.0$ m.

2.3. Flow regime transition analysis

Although the flow transition from the homogeneous to the transition flow regime does not happen instantaneously [1], the definition of an approximate transition point is helpful for modelling the hydrodynamic of bubble columns. In this study, we employ two methods from the literature for investigating the flow regime transition: (i) the swarm velocity and (ii) the drift flux method.

2.3.1. Swarm velocity method

The swarm velocity method was proposed by Zuber and Findlay [22] and is based on the evaluation of the swarm velocity, U_{swarm} :

$$U_{swarm} = U_G / \varepsilon_G \quad (2)$$

In this method, the swarm velocity is plotted against the superficial gas velocity: U_{swarm} is constant in the homogeneous flow regime and starts to increase - at a certain transition superficial velocity, U_{trans} - as the system enters the transition/heterogeneous flow regime. The appearance of the first large bubble is responsible for the increase in the swarm velocity and is an indication of flow regime transition. This method was employed also by Krishna et al. [23], Letzel et al. [24] and Gourich et al. [25], Ribeiro and Mewes [11] and Besagni et al. [2, 9-15].

2.3.2. Wallis plot method

The drift-flux method was proposed by Wallis [26] and was widely used in the literature [2, 12-15, 26, 27]. This method is based on the drift flux (that represents the gas flux through a surface moving with the speed of the two-phase mixture) and it is experimentally obtained as follows:

$$J_T = U_G (1 - \varepsilon_G) \quad (3)$$

Theoretically, the drift flux is written in terms of a parameter, U_b , whose dependence upon ε_G varies with the prevailing flow regime:

$$J_E = U_b (1 - \varepsilon_G) \quad (4)$$

The idea is to employ a model for U_b valid for the homogeneous flow regime and to plot J_E and J_T in the same graph as a function of ε_G . In the homogeneous flow regime J_E is equal to J_T and the transition point is, thus, defined when:

$$J_T \neq J_E \quad (5)$$

The evaluation of U_b is a matter of discussion in the literature, as different models were proposed and applied. In this study, we follow the approach of Krishna et al. [28], which is based on the empirical model of Richardson and Zaki [29]:

$$U_b = u_\infty (1 - \varepsilon_G)^{n-1} \quad (6)$$

where n is fluid-dependent ($n \cong 2$ for water) and u_∞ - the terminal velocity of an isolated bubble - should be fitted with the aid of the experimental data in the determination of the flow regime transition point. Combining Eq. (4) and Eq. (6) results:

$$J_E = u_\infty \varepsilon_G (1 - \varepsilon_G)^n \quad (7)$$

3. The gas holdup data

3.1. Air-water

Figure 3 displays the gas holdup measurements for the air-water system. At low superficial gas velocities, the relationship between the gas holdup and the superficial gas velocity is linear, followed by a change in tendency at a transition superficial gas velocity, U_{trans} . The linear trend corresponds to the homogeneous flow regime and the change in tendency is due to flow regime transition toward the transition flow regime. Indeed, above the transition velocity, “*coalescence-induced-bubbles*” begin to appear, and the bubble coalescence increases the average rise velocity and reduces the gas residence time in the column, thus reducing the gas holdup versus gas velocity slope. It is worth noting that the homogeneous flow regime, in the present bubble column, is characterized by poly-dispersed BSDs and, therefore, it is classified as a “*pseudo-homogeneous*” flow regime [2]. The shape of the gas holdup curve is the one typically found for similar sparger geometries: the sparger used in this study has “*large*” holes ($d_0 > 1$ mm) and, as expected, no peak can be observed in the gas holdup curve [3].

Upon increasing the liquid flowrate, a faster increase in the gas holdup is observed at low U_G , and the transition point also moves toward lower superficial gas velocities. This change is explained by the effect of the liquid flow, which slows down the rise of the bubbles, leading to higher gas holdup: the more compact arrangement of the bubbles leads to an earlier flow regime transition. Our results prove that the counter-current mode has an influence on the gas holdup, as widely discussed in [2], and in agreement with the literature [30-33]. The reader may refer to our previous paper for a comprehensive discussion concerning the hydrodynamic of the system [2].

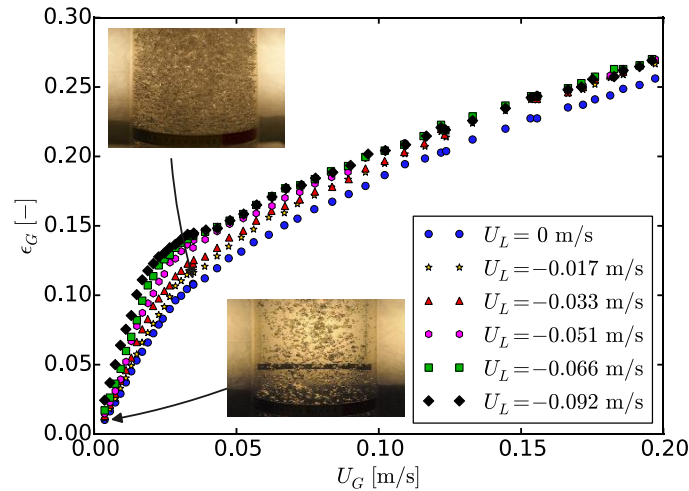


Figure 3. Gas holdup – air-water (influence of the counter-current mode).

3.2. Air-water-NaCl

Most electrolytes inhibit bubble coalescence in water [34-38] and, in this respect, a key concept is the transition concentration, c_t , defined as the concentration above which bubble coalescence is drastically reduced [37, 38]. In the case of NaCl, the threshold is $c_t = 0.145$ mol/l [9]. Depending on the concentration of the electrolyte, we may define a “*coalescent flow regime*” ($c/c_t \leq 1$) and a “*non-coalescent flow regime*” ($c/c_t > 1$); in the present study, five NaCl concentrations ($0 \leq c/c_t \leq 1.17$, in both the “*coalescent flow regime*” and the “*non-coalescent flow regime*”) were tested: Figure 4 displays the gas holdup measurements for the air-water-NaCl system.

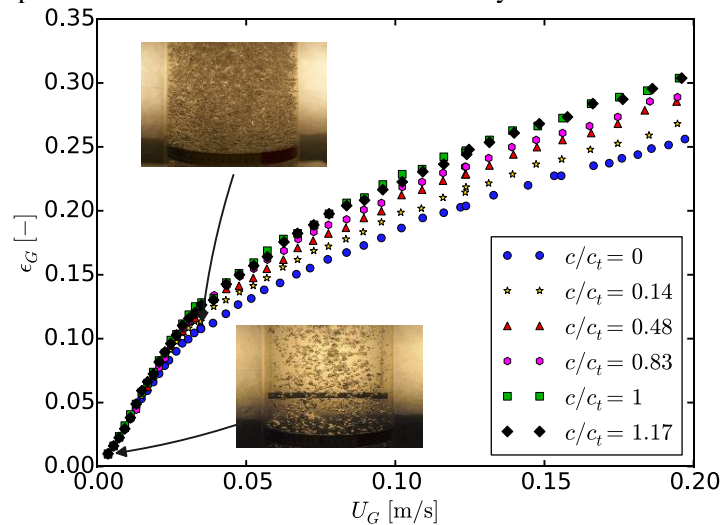


Figure 4. Gas holdup – air-water-NaCl.

The addition of NaCl, up to the critical concentration, increases continuously the gas holdup and stabilizes the homogeneous flow regime due to the coalescence inhibition effect [16, 39]. Above the critical concentration, there is no remarkable difference in the gas holdup and flow regime transition. An interesting aspect is the non-linearity of the electrolytes effect upon the gas holdup. The curve for $c/c_t = 0.14$ and 0.48 is already shifted to considerably higher ε_G values in comparison to the curve related to $c/c_t = 0$, while the relative distance between the curves associated with $c/c_t = 0.48, 0.83$ and 1 is considerably lower. The literature agrees that the increase in gas holdup is a consequence of the homogeneous flow regime stabilization, which is further discussed in Section 4. Further details on the global and local flow properties were presented by Besagni and Inzoli [13].

3.3. Air-water-EtOH

The alcohol molecules are composed of hydrophilic and hydrophobic parts that are adsorbed at the interface when dissolved in water, causing the coalescence suppression [40]. In the present case, the addition of ethanol stabilizes the homogeneous flow regime, due to the coalescence inhibition effect of alcoholic solutions, and, as a consequence (Section 4), increases the gas holdup (Figure 5). Moreover, the addition of ethanol changes the bubble shape and size distributions: we have observed an increased number of small and spherical bubbles (Figure 6b) [14]. It is worth noting that the difference between the two gas holdup curves increases with increasing U_G . Further details on the global flow properties and the bubble size distributions were presented by Besagni et al. [14].

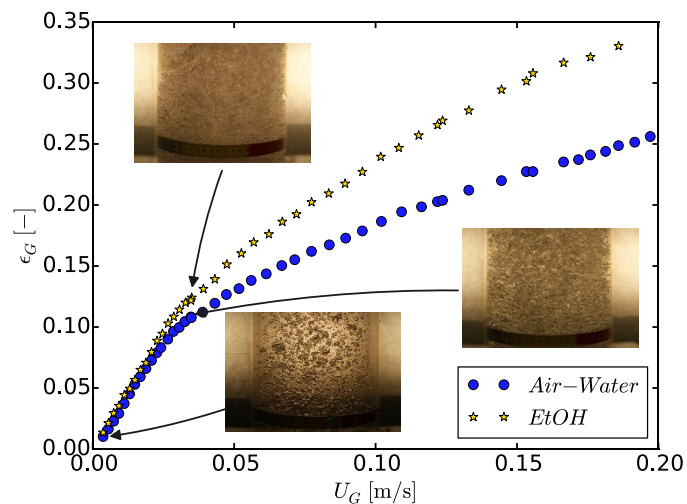
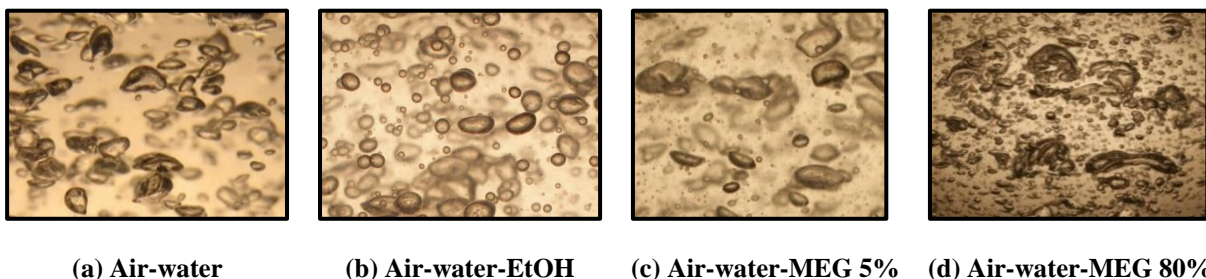


Figure 5. Gas holdup – air-water-EtOH.



(a) Air-water

(b) Air-water-EtOH

(c) Air-water-MEG 5%

(d) Air-water-MEG 80%

Figure 6. Influence of the liquid phase properties on the bubble shapes.

3.4. Air-water-MEG

Figure 7 displays the gas holdup measurements for the air-water-MEG system. The gas holdup continuously increases by increasing the MEG concentration up to $c_{MEG,wt} = 5\%$ ($\mu_L = 1.01$ mPa·s, Figure 7a), along with the contribution of small bubbles (Figure 6c). On the other hand, if the concentration is further increased from $c_{MEG,wt} = 5\%$ ($\mu_L = 1.01$ mPa·s) to $c_{MEG,wt} = 80\%$ ($\mu_L = 7.97$ mPa·s), the gas holdup decreases (Figure 7b). For this last concentration, the gas holdup curve lies even below that obtained for pure water: indeed, increasing the viscosity, the tendency to coalescence prevails, creating large cap-bubbles (Figure 6d) rising the column at a higher velocity, thus reducing the gas holdup. A similar behaviour was observed in the early study of Wilkinson et al. [41] and in more recent studies [42]. In addition, at high viscosity and high U_G “coalescence-induced” bubbles, rising the column, were observed. An interesting discussion concerning the contribution of the “coalescence-induced” bubbles to the gas holdup structure in highly viscous liquid phases was proposed by Yang et al. [43]. Further details on the global flow properties and the bubble size distributions were presented by Besagni et al. [15].

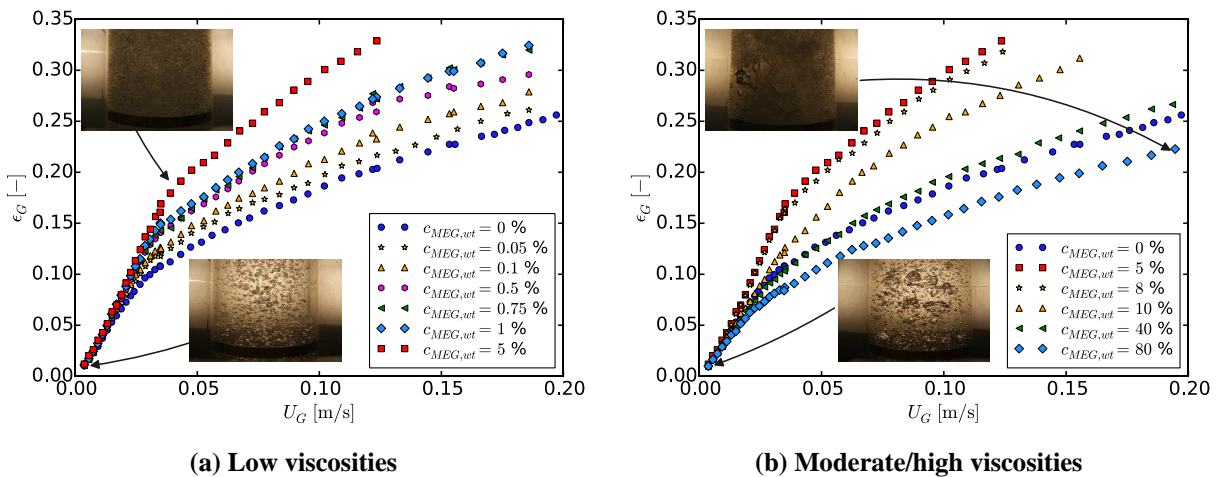


Figure 7. Gas holdup – air-water-MEG.

4. The flow regime transition

The flow regime transition points were investigated by the methods presented in Section 2.3. The values of the transitional gas velocities (U_{trans}) and transitional gas holdups (ϵ_{trans}) are in agreement between the two methods and, following the proposal of Ribeiro and Mewes [39] and Besagni and Inzoli [2], the transition points were evaluated as the mean of the two values. The results of the analysis are presented in Figure 8 and are summarized below:

- **air-water-NaCl.** The homogeneous flow regimes is stabilized while increasing the electrolyte concentration till the critical concentration;
- **air-water-EtOH.** The homogeneous flow regimes is stabilized by the addition of EtOH;
- **air-water-MEG.** The addition of MEG stabilizes or destabilizes the homogeneous flow regime depending on the MEG concentration: the low viscosities stabilizes the homogeneous flow regime, whereas moderate/high viscosities destabilize the homogeneous flow regime.

Regardless of the liquid phase considered, it is interesting to observe the relationship between the homogeneous flow regime stabilization (or destabilization) and the gas holdup increase (or decreasing): if the homogeneous flow regime is stabilized/destabilized, the gas holdup increases/decreases. It has not escaped our notice that the flow regime transition is related to the prevailing BSDs of the system. The detailed discussion of the BSDs is beyond the scope of this paper and the interested reader should refer to the experimental results presented in refs. [14, 15].

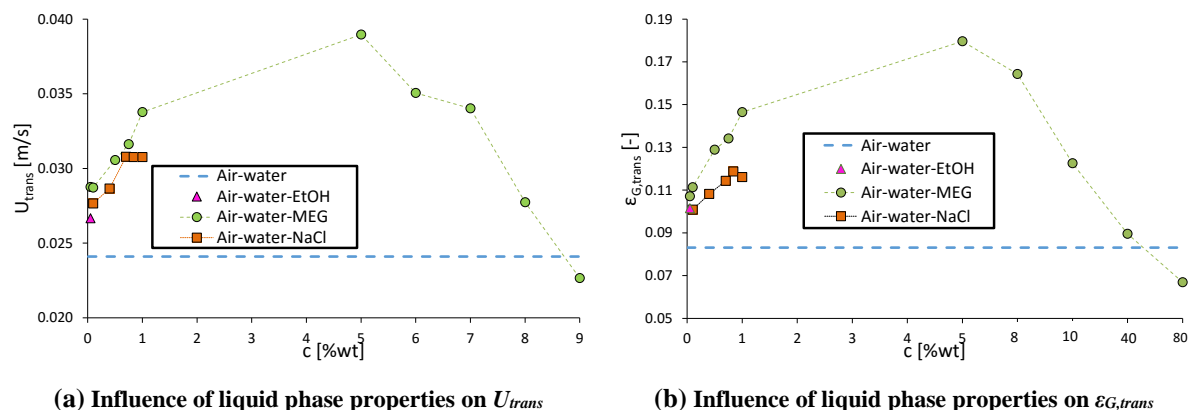


Figure 8. The flow regime transitions: influence of the liquid phase properties.

The experimental results suggest that a change in the liquid phase properties mainly affect the bubble interfacial properties, thus resulting in change in the bubble size distributions (i.e., the balance between coalescence and break-up) and, finally, changing the gas holdup curve. This concept was firstly proposed by Besagni [44] and has been further discussed by Besagni et al. [14-15]. The above-mentioned relationship between the bubble scale and the laboratory-reactor scale may be governed by the lift force. In particular, the lift force induces the changes in the bubble size distributions and affects the motion of the small and large bubbles [2, 15]. In this respect, the lift force affects the bubble column fluid dynamics and the flow regime transitions. The larger bubbles, having a negative lift coefficient, move toward the center of the pipes, thus, promoting the “*coalescence-induced*” bubble and the flow regime transition. On the contrary, the small bubbles, having positive lift coefficient, stabilize the homogeneous flow regime. This concept has been widely discussed and verified in our previous paper [15], with respect to the MEG system. Of course, this concept should be verified in future studies with respect to other systems (i.e., air water and active agent systems).

5. Conclusions

We have experimentally investigated the influence of liquid phase properties on gas holdup and flow regime transition in a large-scale counter-current bubble column. The bubble column is 5.3 m in height, has an inner diameter of 0.24 m, it was operated with gas superficial velocities in the range of 0.004–0.20 m/s and, in the counter-current mode, the liquid was recirculated up to a superficial velocity of -0.09 m/s. Air was used as the dispersed phase and various fluids were employed as liquid phases. The experimental dataset consist in gas holdup measurements and was used to investigate the global fluid dynamics and the flow regime transition between the homogeneous and the transition flow regimes. We found that the liquid velocity and the liquid phase properties significantly affect the gas holdup and the flow regime transition. The experimental results suggest that a change in the liquid phase properties affect the bubble interfacial properties, thus resulting in change in the bubble size distribution and, finally, changing the gas holdup curve. A stabilization/destabilization of the homogeneous flow regime results in an increase/decrease of the gas holdup increase (or decreasing). The relationship between the bubble scale and the laboratory-reactor scale may be governed by the lift force. Further studies should focus on the lift force as the link between the bubble scale and the laboratory-reactor scale; in this respect, extensive experimental campaigns to obtain information on bubble sizes and shapes should be performed. Possibly, the lift force may be included, in future studies, in gas holdup correlations to link the local and the global scales.

6. Acknowledgment

The authors wish to express their thanks to Itecond srl and to Ing. Luca Primavesi, in particular, for having supplied monoethylene glycol for the experimental campaign.

References

- [1] Nedeltchev S 2015 *Chem. Eng. Sci.* **137** 436-44
- [2] Besagni G and Inzoli F 2016 *Chem. Eng. Sci.* **146** 259–290
- [3] Sharaf S, Zednikova M, Ruzicka M C and Azzopardi B J 2015 *Chem. Eng. J.* **288** 489–504
- [4] Kataoka I and Ishii M 1987 *Int. J. Heat Mass Tran.* **30** 1927-39
- [5] Mudde R F, Hartevelde W K and van den Akker H E A 2009 *Ind. Eng. Chem. Res.* **48** 148-159
- [6] Ruzicka M C, Drahoš J, Fialová M and Thomas N H 2001 *Chem. Eng. Sci.* **56** 6117-24
- [7] Shah Y T, Kelkar B G, Godbole S P and Deckwer W D 1982 *AIChE J.* **28** 353-379
- [8] Shaikh A. and Al-Dahhan M. 2013. *Ind. Eng. Chem. Res.* **52** 8091-8108
- [9] Besagni G and Inzoli F 2016 *Chem. Eng. Sci.* **145** 162–180
- [10] Besagni G, Guédon G and Inzoli F 2014 *J. Phys Conf Ser* **547** 012024
- [11] Besagni G, Guédon R G and Inzoli F 2016 *ASME J. Fluids Eng* **138** 011302-15
- [12] Besagni G and Inzoli F 2016 *Ext. Therm. Fluid. Sci.* **74** 27–48
- [13] Besagni G and Inzoli F 2015 *J. Phys Conf Ser* **655** 012039
- [14] Besagni G, Inzoli F, De Guido G and Pellegrini A M 2016 *Chem. Eng. Res. Des.* **112** 1-15
- [15] Besagni G, Inzoli F, De Guido G and Pellegrini A M 2016 *Chem. Eng. Sci.* **158** 509-538
- [16] Zahradnik J, Fialova M, Rruzivc k, M., Drahovs, J., Kavstanek F and Thomas N H 1997 *Chem. Eng. Sci.* **52** 3811-26
- [17] Kestin J, Sokolov M and Wakeham W A 1978 *J. Phys. Chem. Ref. Data* **7** 941-948
- [18] Vargaftik N, Volkov B and Voljak L 1983 *J. Phys. Chem. Ref. Data* **12** 817-820
- [19] Perry R H and Green D W 2008 *Perry's chemical engineers' handbook* (New York)
- [20] Sun T and Teja A S, K 2003 *J. Chem. Eng. Data* **48** 198-202
- [21] MEGlobalTM 2015 *Ethylene Glycol. Product Guide*
- [22] Zuber N and Findlay J A 1965 *J. Heat Transf* **87** 453-68
- [23] Krishna R, Wilkinson P M and Van Dierendonck L L 1991 *Chem. Eng. Sci.* **46** 2491-6
- [24] Letzel H M, Schouten J C, van den Bleek C M and Krishna R 1997 *Chem. Eng. Sci.* **52** 3733-9
- [25] Gourich B, Vial C, Essadki A H, Allam F, Belhaj Soulami M and Ziyad M 2006 *Chem. Eng. Process.* **45** 214-23
- [26] Wallis G B 1969 *One-dimensional two-phase flow* (New York)
- [27] Passos A D, Voulgaropoulos V P, Paras S V and Mouza A A 2015 *Chem. Eng. Res. Des.* **95** 93-104
- [28] Krishna R, Ellenberger J and Maretto C 1999 *Int. Commun. Heat Mass* **26** 467-75
- [29] Richardson J F and Zaki W N 1997 *Chem. Eng. Res. Des.* **75**, Supplement S82-S100
- [30] Otake T, Tone S and Shinohara K 1982 *J. Chem. Eng. Jpn.* 338–340
- [31] Baawain M S, El-Din M G and Smith D W 2007 *Ozone: Sci. Eng.* **29** 343–352
- [32] Biń A K, Duczmal B and Machniewski P 2001 *Chem. Eng. Sci.* **56** 6233–6240
- [33] Jin H, Yang S, He G, Wang M and Williams R A 2010 *J. Chem. Technol. Biot.* **85** 1278–1283
- [34] Craig V S J, Ninham B W and Pashley R M 1993 *J. Phys. Chem-US* **97** 10192-7
- [35] Deschenes L A, Barrett J, Muller L J, Fourkas J T and Mohanty U 1998 *J. Phys. Chem B* **102** 5115-9
- [36] Keitel G and Onken U 1982 *Chem. Eng. Sci.* **37** 1635-8
- [37] Lessard R R and Zieminski S A 1971 *Ind. Eng. Chem. Fund.* **10** 260-9
- [38] Marrucci G and Nicodemo L 1967 *Chem. Eng. Sci.* **22** 1257-65
- [39] Ribeiro Jr C P and Mewes D 2007 *Chem. Eng. Sci.* **62** 4501-9
- [40] Albijanić B, Havran V, Petrović D L, Durić M and Tekić M N 2007 *AIChE J.* **53** 2897-2904
- [41] Wilkinson P M, Spek A P and van Dierendonck L L 1992 *AIChE J.* **38** 544-54
- [42] Rabha S, Schubert M and Hampel U 2014 *AIChE J.* **60** 3079-3090
- [43] Yang J H, Yang J I, Kim H J, Chun d H, Lee H T and Jung H 2010 *Chem Eng Process.* **49** 1044-1050
- [44] Besagni G 2016 *Bubble column fluid dynamics: experimental and numerical investigations* Ph.D. Thesis, Politecnico di Milano